Chromospheric evaporation flows and density changes deduced from Hinode/EIS during an M1.6 flare

P. Gömöry[1], A. M. Veronig[2], Y. Su[2,3], M. Temmer[2], J. K. Thalmann[2]

[1] Astronomical Institute, Tatranská Lomnica, Slovakia
[2] IGAM/Institute of Physics, University of Graz, Graz, Austria
[3] Key Laboratory of Dark Matter & Space Astronomy, Purple Mountain Observatory, Nanjing, China

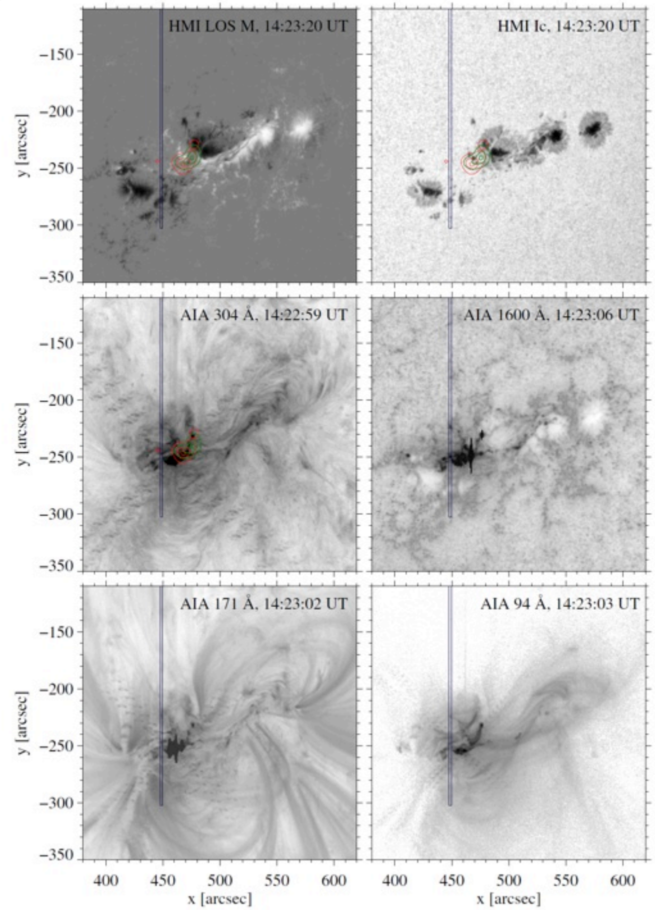

Introduction

- standard eruptive flare model:
  - energy to power flares stored in nonpotential coronal magnetic fields
  - magnetic reconnection → energy released in the corona converted into local heating and accelerating particles
  - accelerated particles → guided by the ambient magnetic field and progress downward to the denser environment → energy dissipated by Coulomb collisions
  - chromospheric plasma heated to coronal T → expanding upward → process known as **chromospehric evaporation**

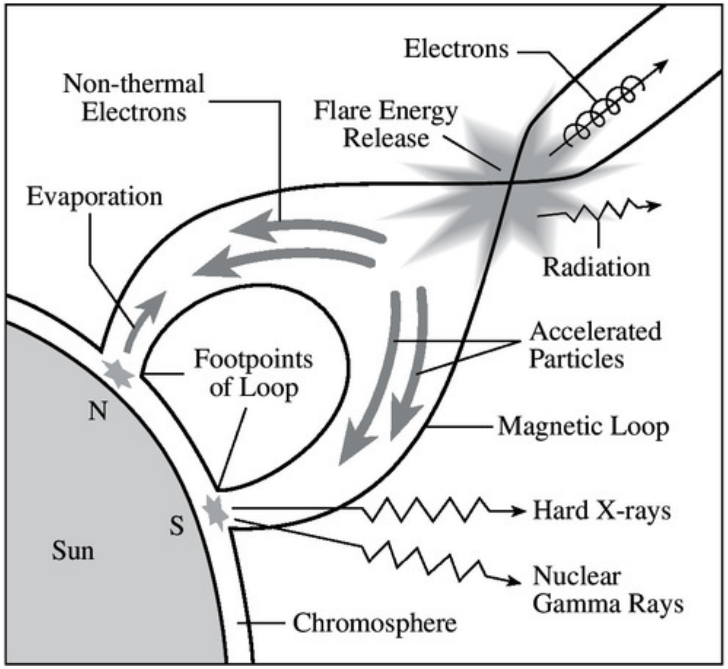

- hydrodynamic simulations:
  - two evaporation regimes separated by an energy flux density threshold → ~10^{10} erg cm^{-2} s^{-1} (Fisher et al. 1985, ApJ 289, 414)
  - **gentle evaporation:** deposited energy lower than threshold → heated material slowly expands upward (velocities: several tens of km s^{-1})
  - **explosive evaporation:** deposited energy higher than threshold → radiative cooling insufficient → plasma rapidly heated → local gas pressure rises → explosive upward expansion (velocities: several hundred km s^{-1})
    but, to regain momentum balance → the cooler material is pushed downward

Data and data reduction

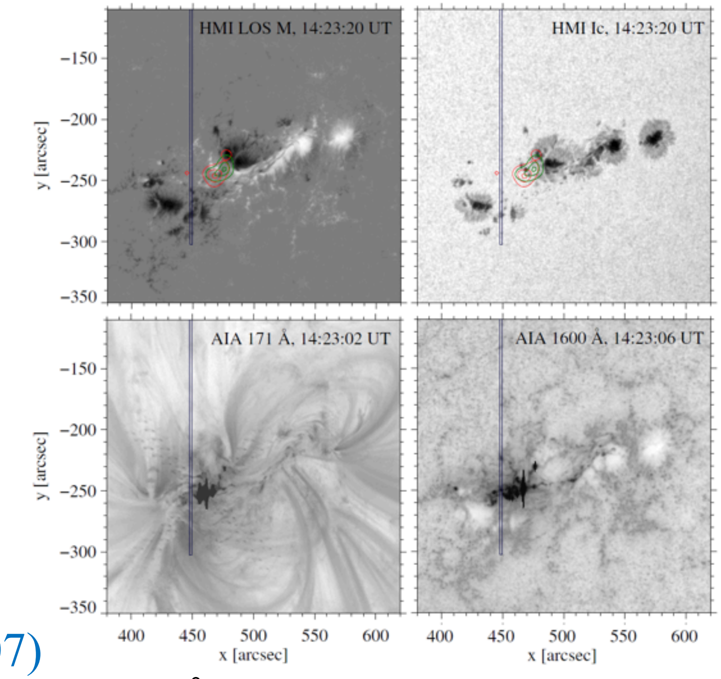

- observing program: HOP-180
- date: February 16, 2011
- time: 13:38 – 15:43 UT
- target: active region 11158
- position: x ~ 500”; y ~ -250”
- **M1.6 flare and EIT wave captured**

Instruments:

- Hinode/EIS (Culhane at al. 2007, Sol. Phys. 78, 107)
  - EUV spectra → selected spectral lines: Fe XIII 202.044 Å (log T = 6.2)
    Fe XVI 262.980 Å (log T = 6.4)
  - slit parameters: 2” width and 512” height
  - exposure time: 45 s; cadence: ~ 49 s
  - acquired data: corrected for photometric effects and calibrated (wavelength drift compensated using HK method)
  - spectral profiles fitted by single-Gaussian function → spectral parameters
  - Jeffrey et al. 2016, A&A 590, A99: EIS Fe XVI flare profiles can be confidently fitted with a kappa line profile
- RRHESSI (Lin et al. 2002, Sol. Phys. 210, 3)
  - simultaneous X-ray imaging and spectroscopy (3 – 100 keV)
- SDO/AIA (Lemen et al. 2012, Sol. Phys. 275, 17)
  - context data in several UV and EUV channels

Data and data reduction

- observing program: HOP-180
- date: February 16, 2011
- time: 13:38 – 15:43 UT
- target: active region 11158
- position: x ~ 500”; y ~ -250”
- **M1.6 flare and EIT wave captured**

Instruments:

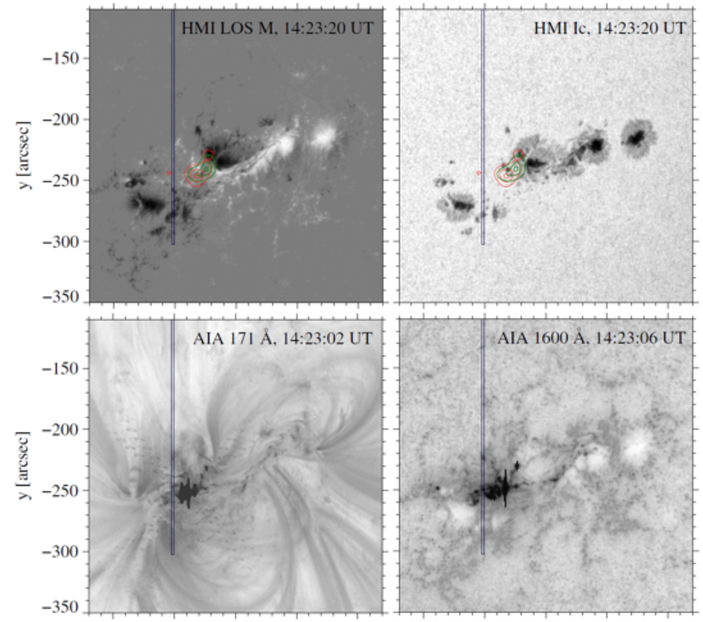

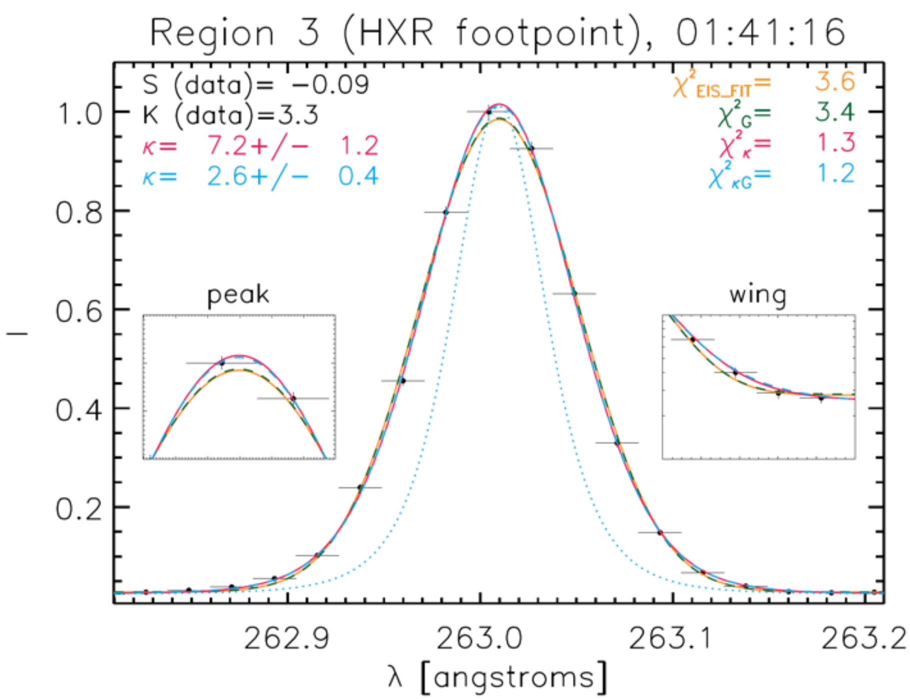

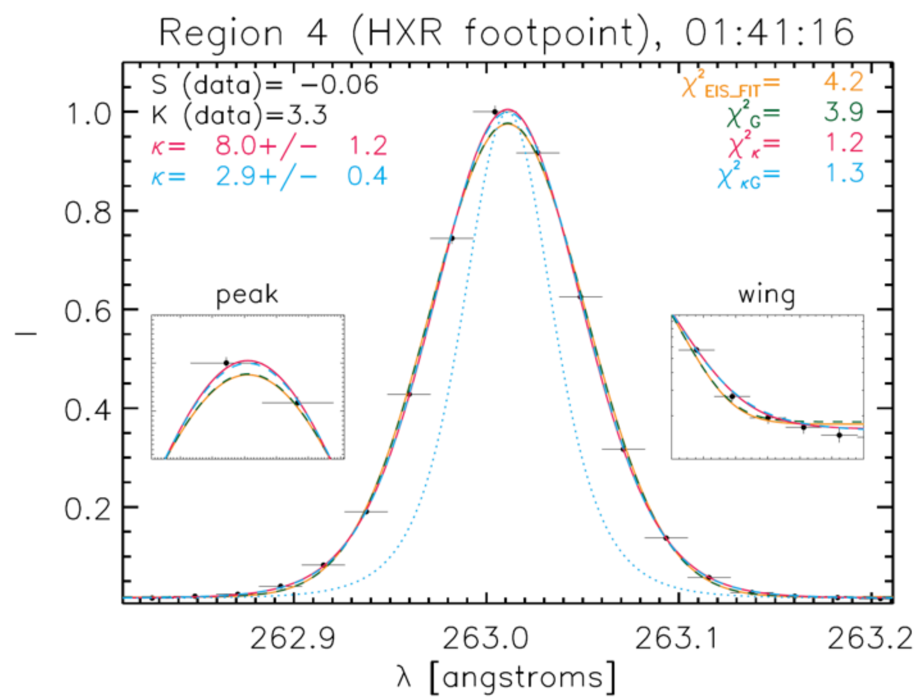

Data and data reduction

- observing program: HOP-180
- date: February 16, 2011
- time: 13:38 – 15:43 UT
- target: active region 11158
- position: x ~ 500”; y ~ -250”
- **M1.6 flare and EIT wave captured**

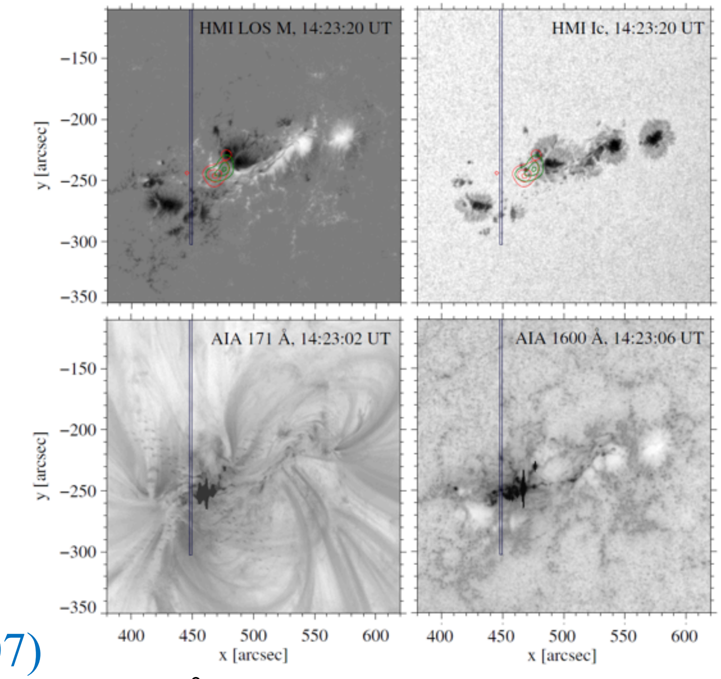

Instruments:

- Hinode/EIS (Culhane at al. 2007, Sol. Phys. 78, 107)
  - EUV spectra → selected spectral lines: Fe XIII 202.044 Å (log T = 6.2)
    Fe XVI 262.980 Å (log T = 6.4)
  - slit parameters: 2” width and 512” height
  - exposure time: 45 s; cadence: ~ 49 s
  - acquired data: corrected for photometric effects and calibrated (wavelength drift compensated using HK method)
  - spectral profiles fitted by single-Gaussian function → spectral parameters
  - Jeffrey et al. 2016, A&A 590, A99: EIS Fe XVI flare profiles can be confidently fitted with a kappa line profile
- RRHESSI (Lin et al. 2002, Sol. Phys. 210, 3)
  - simultaneous X-ray imaging and spectroscopy (3 – 100 keV)
- SDO/AIA (Lemen et al. 2012, Sol. Phys. 275, 17)
  - context data in several UV and EUV channels

Results: event overview

- GOES + RHESSI 3-25 keV
  - start: 14:19 UT; peak: 14:25 UT
- RHESSI 25-100 keV
  - sharp peak at 14:23:38 UT
- main energy deposition occurred 1.5 min before SXR peak → related to the chromospheric evap. flows

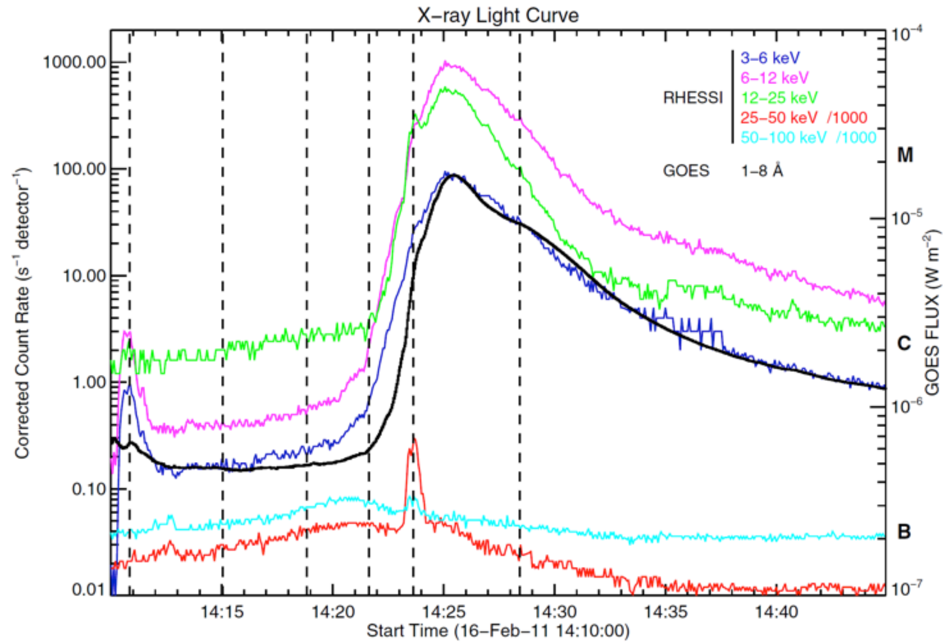

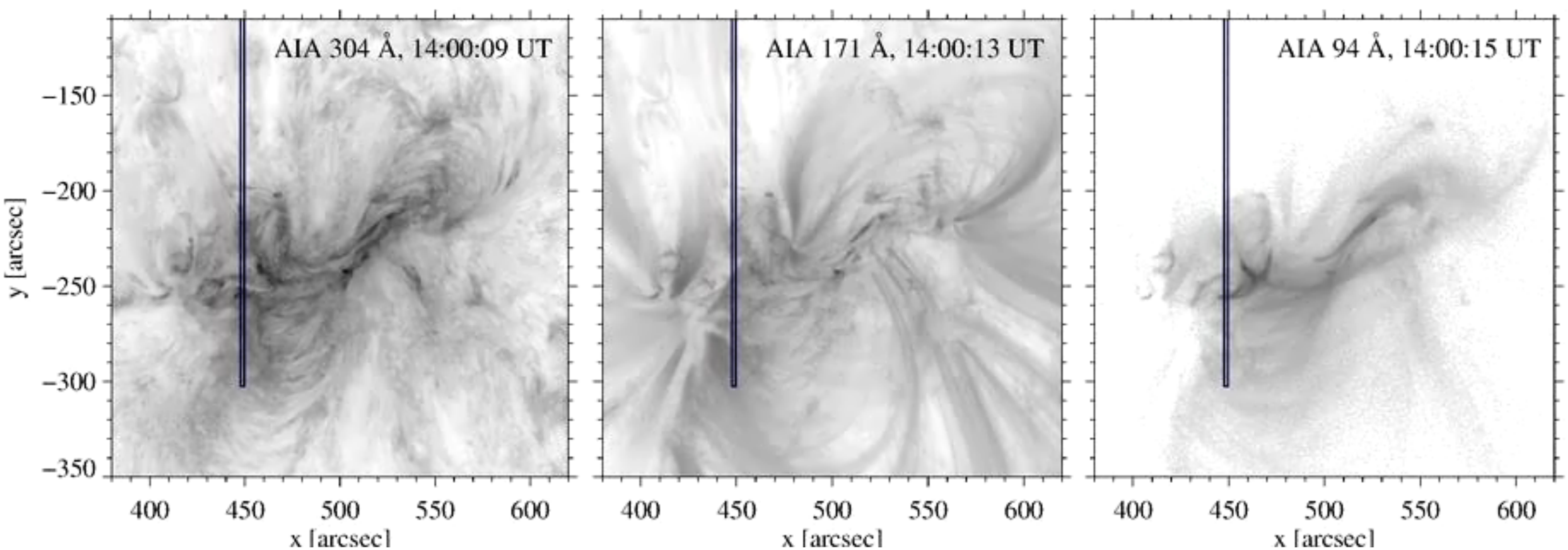

Results: EIS spectroscopy of the flare

- EIS slit co-spatial with the flare kernel
- several events observed: EIT wave, erupting filament, flare
- region of interest: y ~ -260” – -250” → covers eastern flare kernel

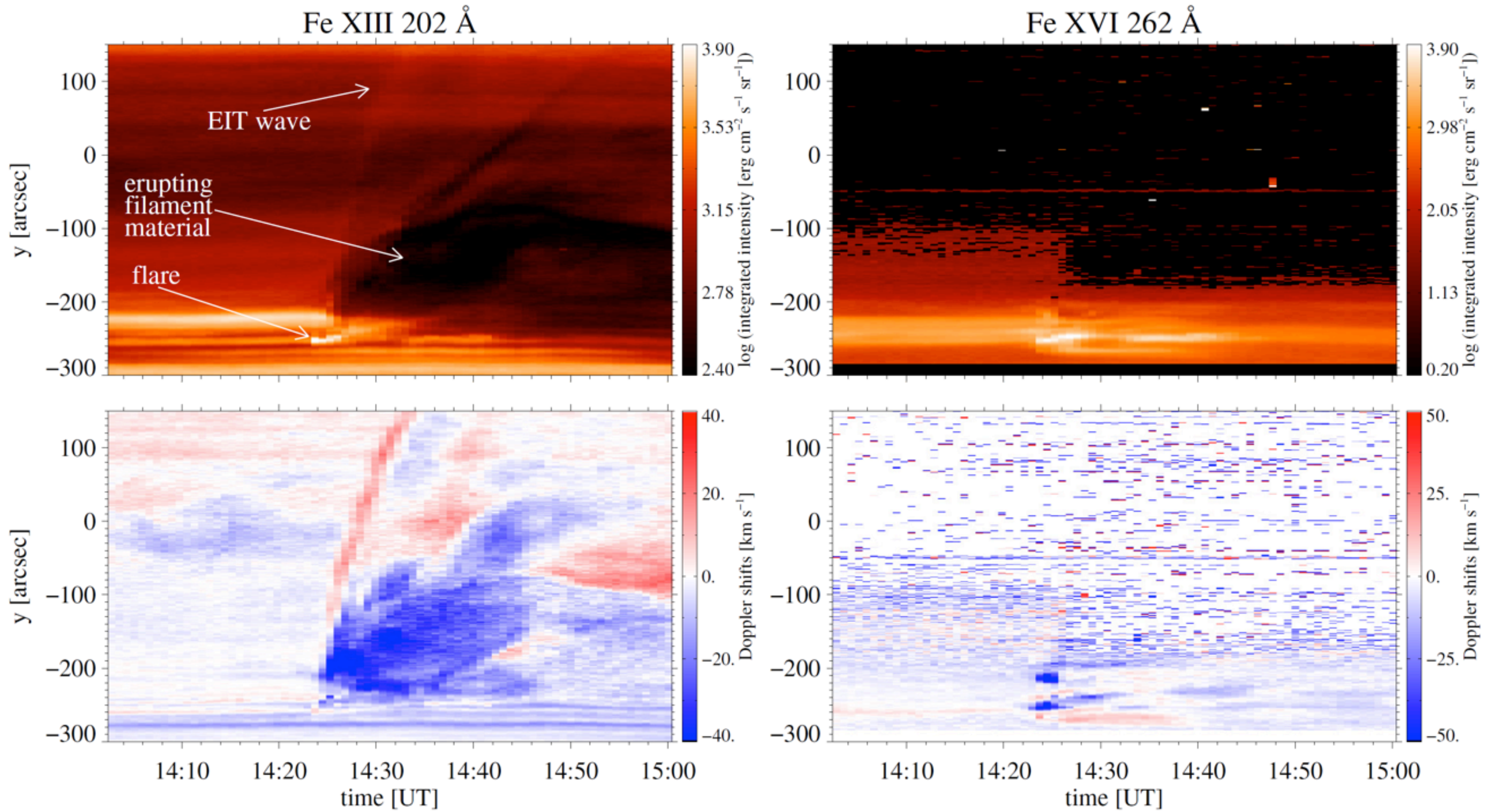

Results: EIS spectroscopy of the flare

- EIS slit co-spatial with the flare kernel
- several events observed: EIT wave, erupting filament, flare
- region of interest: y ~ -260” – -250” → covers eastern flare kernel

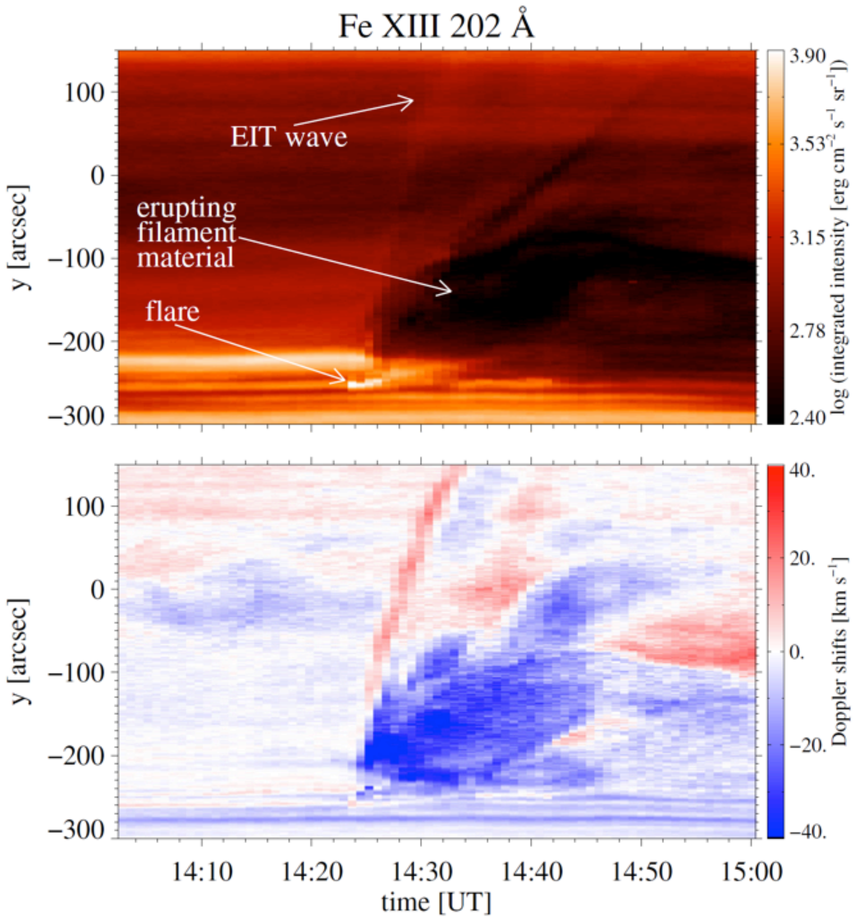

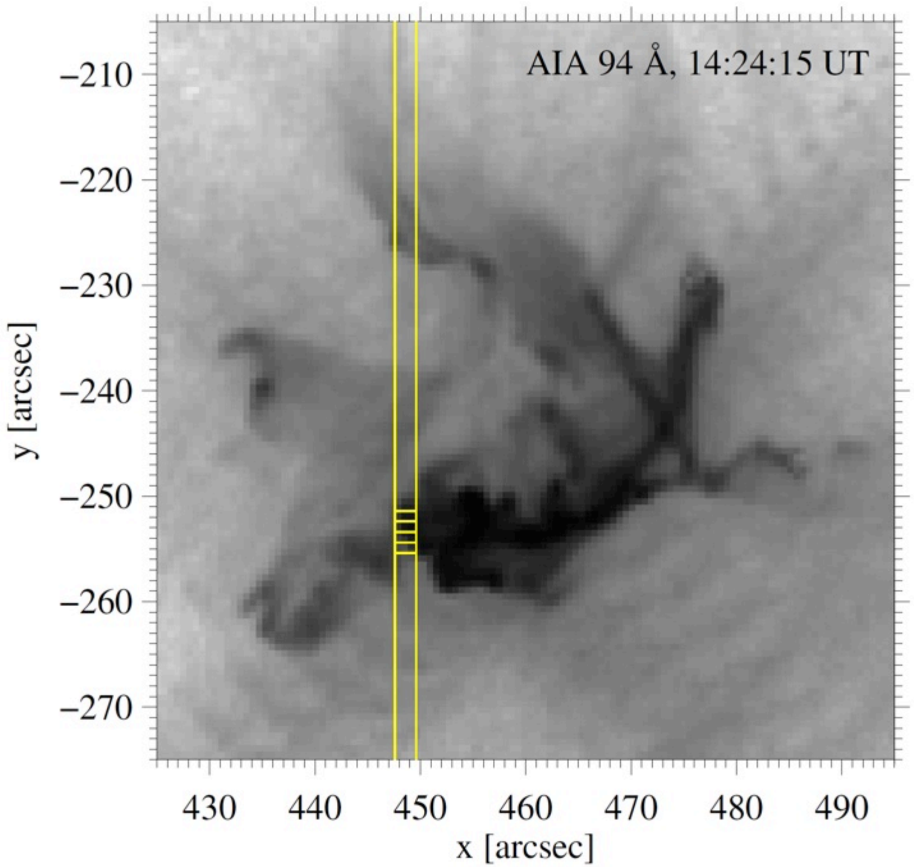

Results: EIS spectroscopy of the flare

- intensity:
  - impulsive phase clearly visible
  - Fe XIII 202 Å reaches its maximum one exposure earlier than Fe XVI 262 Å visible
- Doppler shifts:
  - pre-flare phase →
    Fe XIII: weak blueshifts gradually increasing from ~0 km s^{-1} to ~10 km s^{-1}
    Fe XVI: no obvious Doppler shifts
  - main impulsive phase:
    Fe XIII: only weak redshifts of 2-3 km s^{-1}; detected only for a single exposure → only blueshifts of 10 km s^{-1} detected later
    Fe XVI: only blueshifts; maximum values of ~55 km s^{-1} simultaneously with the intensity peak
    but Fe XVI spectral profiles exhibit clear asymmetry: two-component fit → velocities up to 80-150 km s^{-1}

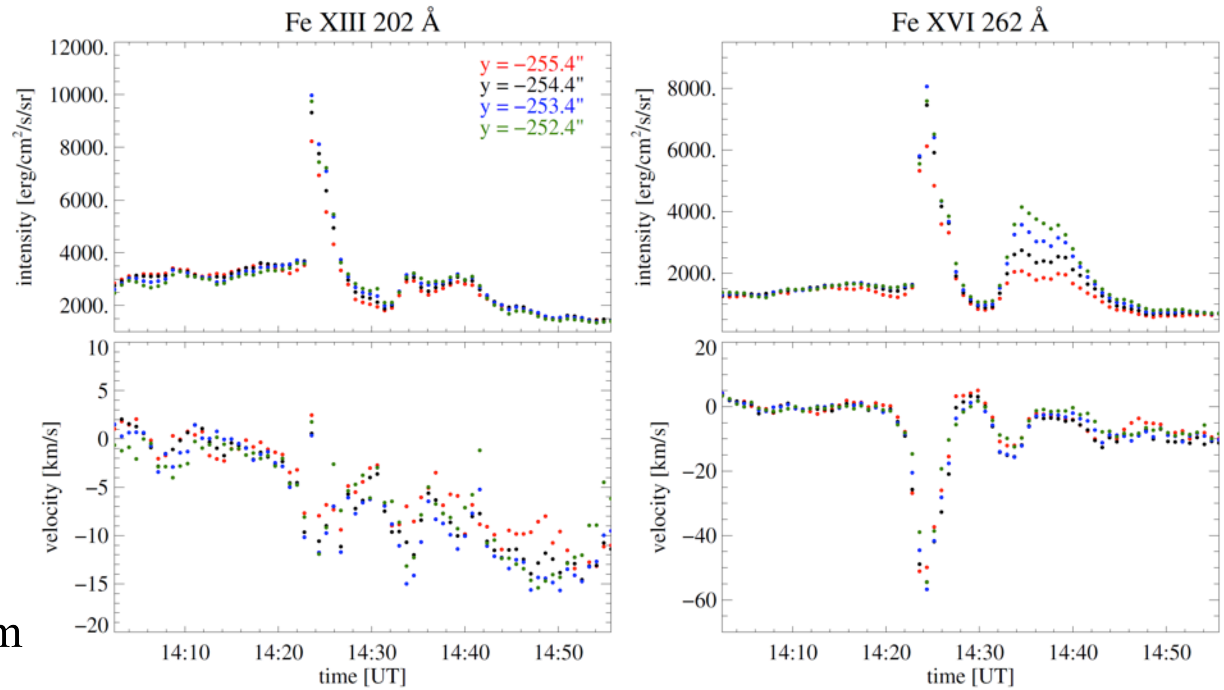

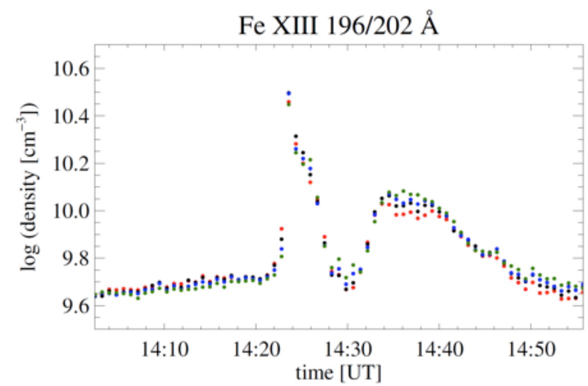

Results: EIS spectroscopy of the flare

- Fe XVI: clear asymmetry visible during the main impulsive phase
- Fe XIII: only single-Gaussian spectral profiles detected
  - intensity increase in the very far blue wing → signature of another spectral line (may by a blend of Fe XI and Fe XII at 201.74 Å)

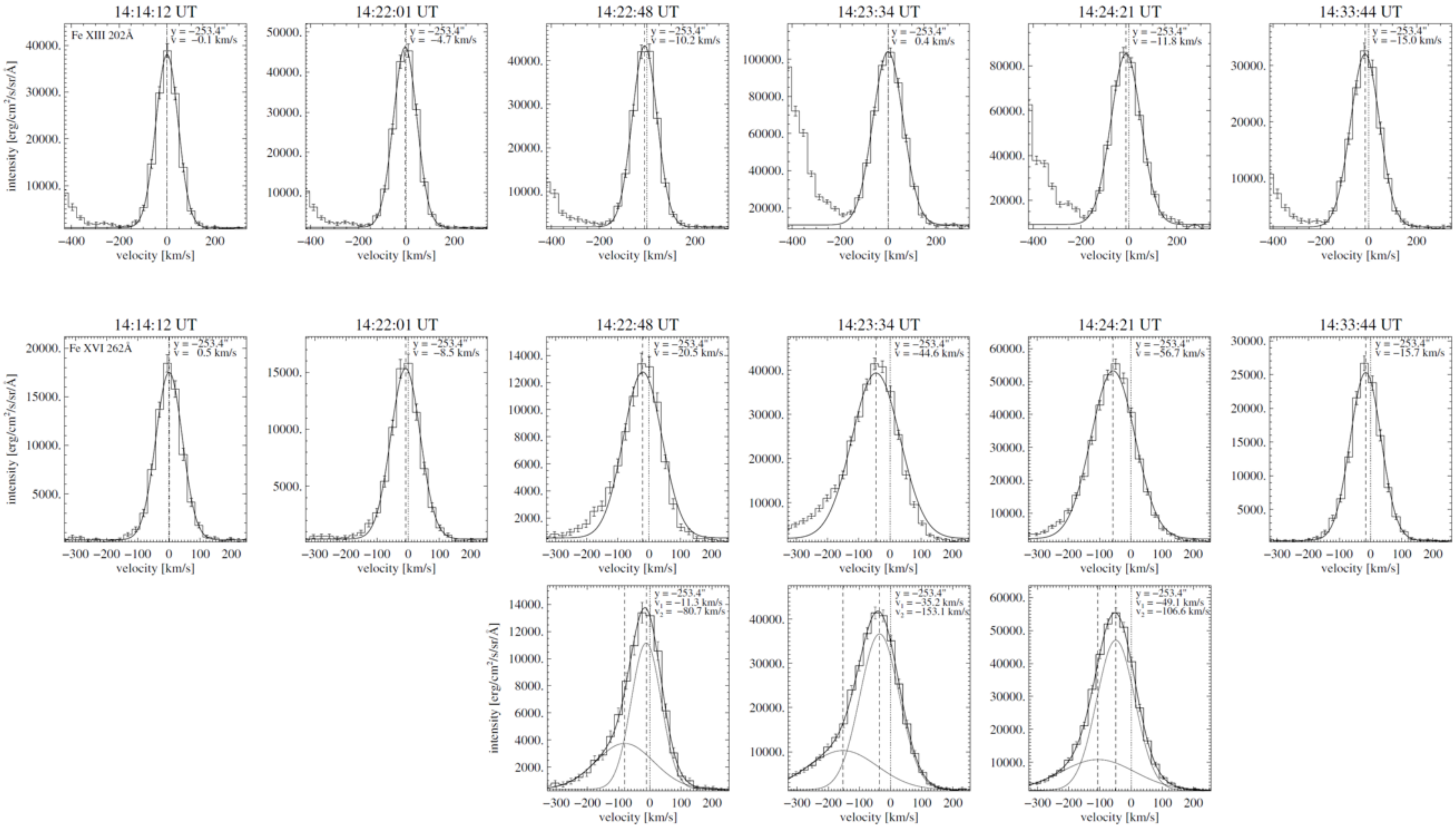

Results: EIS spectroscopy of the flare

- density:
  - derived using Fe XIII 196/202 line pair
  - pre-flare: 5.01×10^{9} cm^{-3} (log $n_e \sim 9.7$)
  - flare peak: 3.16×10^{10} cm^{-3} (log $n_e \sim 10.5$)
  - increase within less than two minutes during the impulsive phase

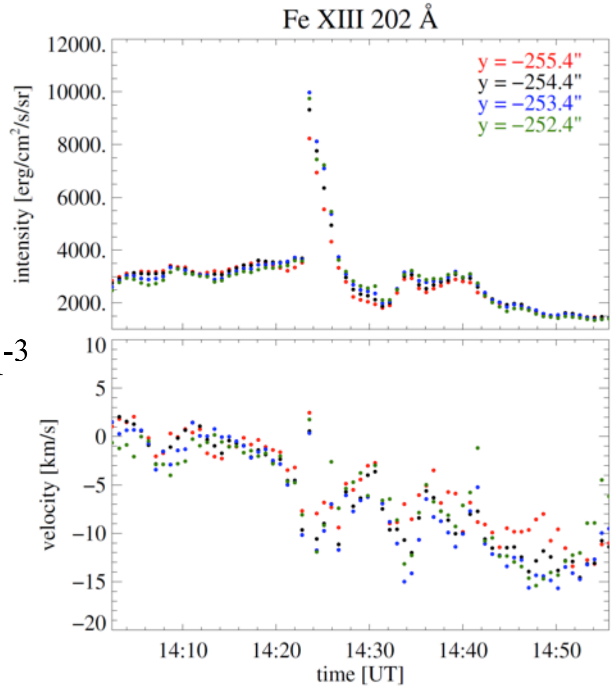

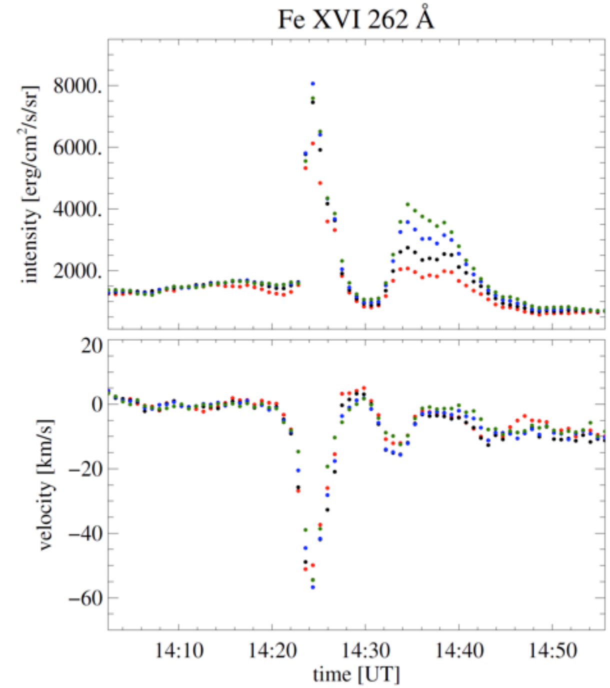

- decline phase:
  - secondary peak observed in all spectral characteristics
  - blueshifts of ~ 15 km s^{-1} detected in both spectral lines
  - detected upflows correspond to significant intensity and density enhancements → density and intensity peaks are delayed, but persist much longer than the corresponding peaks in the Doppler shifts
  - **evidence that expanding hot material that is due to chromospheric evaporation fills the flare loops**

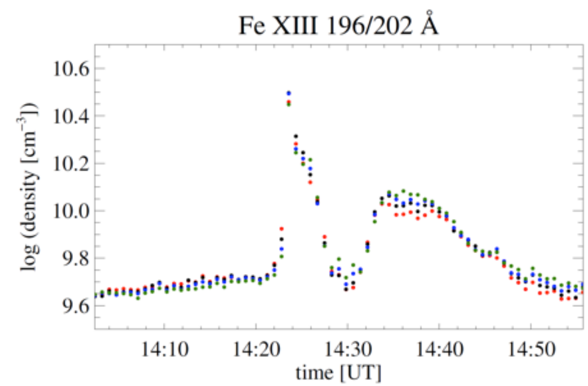

Results: RHESSI X-ray spectroscopy of the flare

– EIS slit co-spatial with the flare kernel

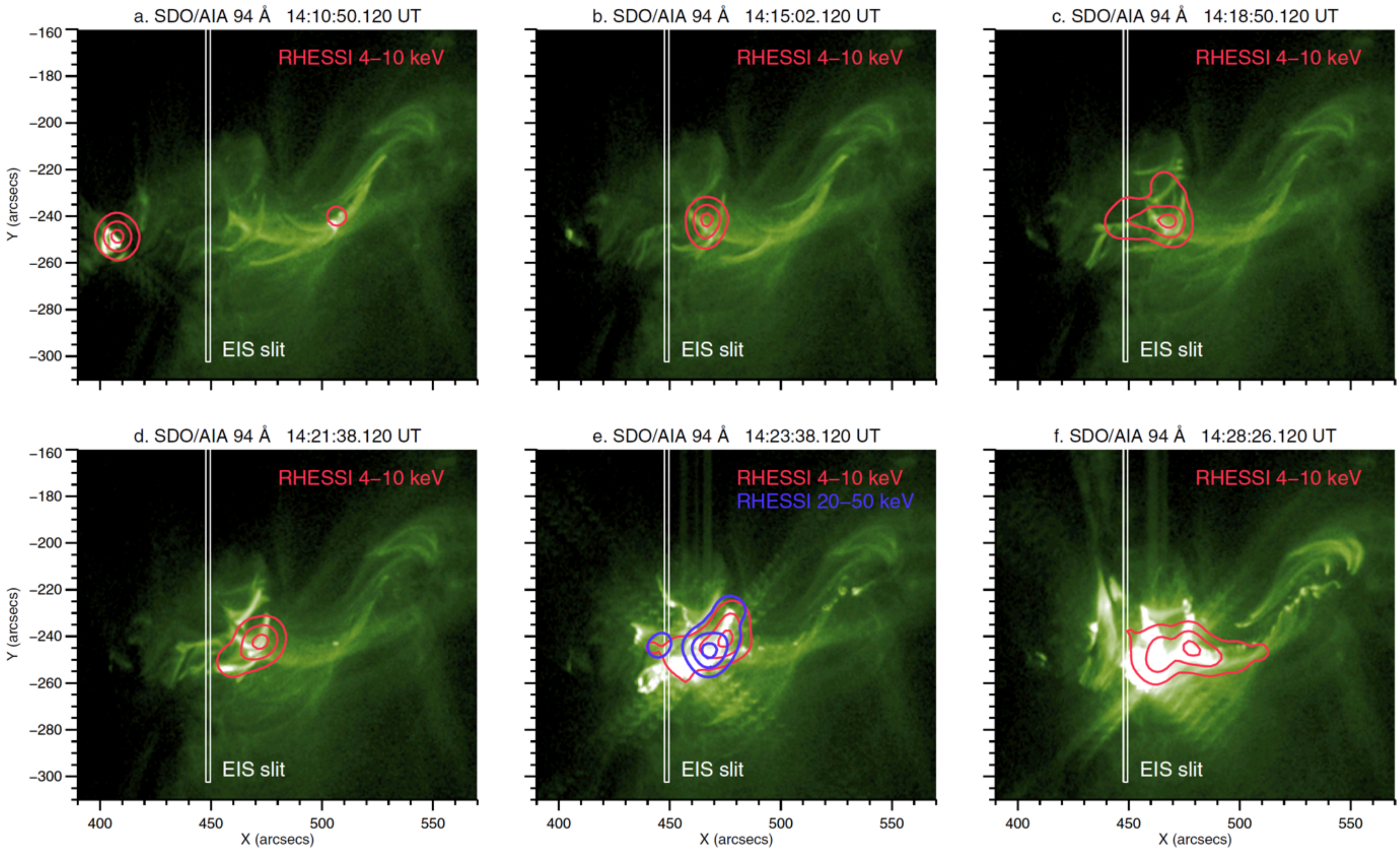

Results: RHESSI X-ray spectroscopy of the flare

- RHESSI spectra for the rising flare phase, HXR peak time, and decay phase
  - fitted with an isothermal component and an nonthermal thick-target model
- fitting results around the HXR peak
  - estimation of the nonthermal energy flux of 7.71×10^{27} erg s^{-1}
  - cross-section of the flaring loops: area enclosed by the 50% contour in the 20-50 keV image
  - **nonthermal energy flux density: 1.34×10^{10} erg s^{-1} cm^{-2}**
  - **low-energy cut-off: ≤ 16 keV**

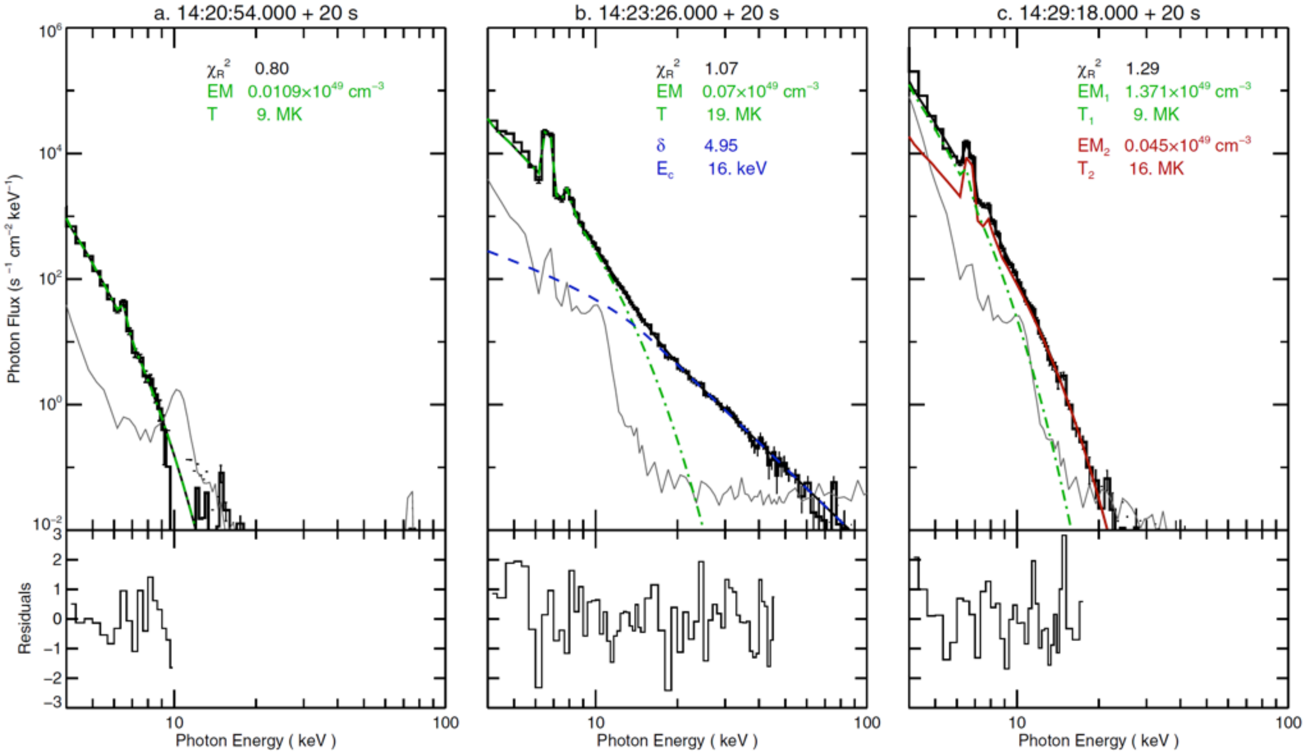

Discussion and conclusions

- spectroscopic observations of the M1.6 flare
  - intensity maxima of the two analysed spectral lines not reached simultaneously, but correspond well with the HXR peak time
  - strong upflows in the Fe XVI 262 Å; no significant flows in the Fe XIII 202 Å

  → **confirmation of a dependency of the Doppler velocity directions on the formation temperature** (Kamio et al. 2005, Milligan et al. 2006, Young et al. 2013)
  - density changes: increase from 5.01×10^{9} cm^{-3} to 3.16×10^{10} cm^{-3} within less than two minutes; obtained values fit previous findings (Graham et al. 2011, Watanabe et al. 2010, Young et al. 2013, Brosius 2013

Results in agreement with the scenario of explosive chromospheric evaporation

- energy flux deposited by the beam of accelerated electrons to the lower atmosphere: only 1.34×10^{10} erg s^{-1} cm^{-2} → value very close to the theoretical threshold of 10^{10} erg s^{-1} cm^{-2} (Fisher et al. 1985) between gentle and explosive evaporation
- estimated low-energy cut-off of ≤ 16 keV
  - hydrodynamical simulations of Fisher et al. (1985) performed under several assumption, e.g., fixed low-energy cut-off = 20 keV → **crucial for comparison with our results**

Discussion and conclusions

- recent hydrodynamic simulations (Reep et al. 2015)
  - the explosive evaporation threshold is dependent on the cut-off energy → threshold could be lower for lower energy cut-offs
  - lower energy electrons are more efficient in heating loops and driving dense plasma into the corona

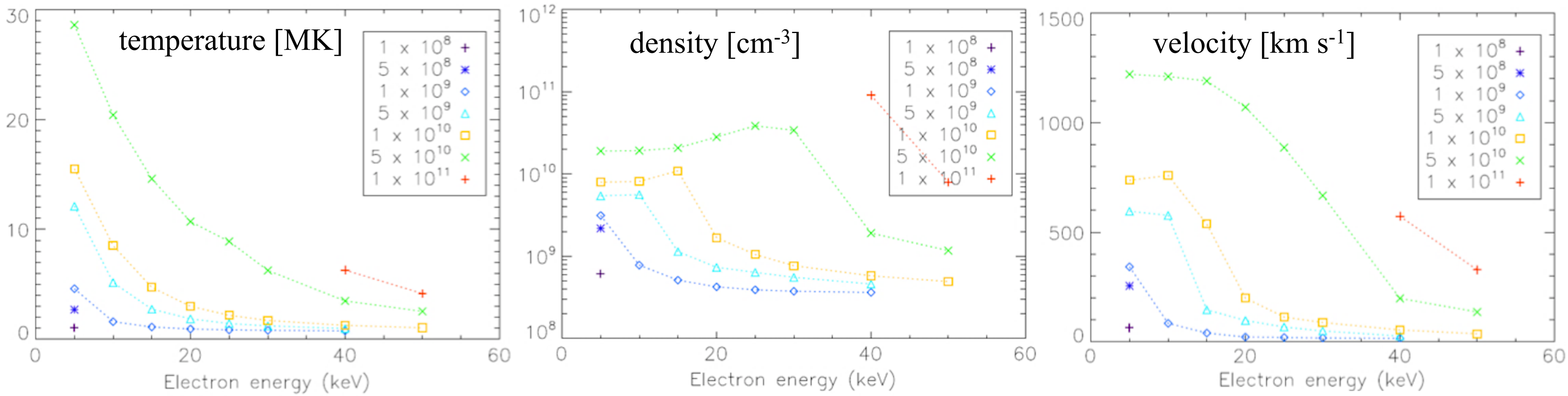

- the response of the flaring atmosphere strongly depends on the properties of the heating electron beams

→ our results provide observational support for this theoretical prediction

Thank you for your attention.

Results: EIS spectroscopy of the filament eruption

- Fe XIII 202 Å: all corresponding spectral profiles exhibit a two-component shape → second component shifted to shorter λ → upflows with velocities of around 250 km s^{-1} – 300 km s^{-1}
- Fe XVI 262 Å: spectra to noisy and weak